

# COG 11.3 New Features

David Heinrichs\*, Edward Lent and Chuck Lee

Lawrence Livermore National Laboratory, 7000 East Avenue, L-198, Livermore, CA 94550, USA

Received: 16 June 2024 / Received in final form: 18 September 2024 / Accepted: 3 October 2024

**Abstract.** COG is a high fidelity, multi-particle, Monte Carlo radiation transport code in development at LLNL since 1980 in support of multiple applications including nuclear criticality safety, radiation shielding, radiography, and subcritical multiplicity analysis. COG 11.3 is the latest version scheduled for public release in 2024 representing the culmination of ten years of development since previous releases. This paper describes the major new features available in COG 11.3 including: (a) updated nuclear data libraries; (b) updated activation data; (c) advanced LLNL Fission Reaction Event Yield Algorithm; (d) new time-tagged list-mode detector feature; (e) new spontaneous fission source feature; (f) new alpha and deuteron particle transport; (g) updated electron transport (implementing EGS5 with internal electron library generation using PEGS5); (h) three new estimators for the effective delayed neutron fraction; (i) new input pre-processor options for user-friendly generation of three-dimensional rectangular and triangular lattice geometries; (j) new parallel-processing capabilities for the inverse reactor period and CritDetVR features using MPI; (k) a new imaging detector feature; and (l) details of the modernized COG website at <https://cog.llnl.gov>. Like previously released versions, COG11.3 will be available to users through RSICC at ORNL, the Nuclear Energy Agency Data Bank at OECD, and by special arrangement through LLNL.

## 1 Introduction

COG is a high fidelity, multi-particle, Monte Carlo, radiation transport code developed at Lawrence Livermore National Laboratory (LLNL) in support of multiple applications including nuclear criticality safety, radiation shielding, radiography, and subcritical multiplicity analysis. COG 11.3 is the next public release and builds on capabilities provided in previously released public versions in 2010–2013; namely, versions 11.1 [1], 11.0 [2], 10 [3]. This paper describes the new features available in version 11.3.

## 2 New features

### 2.1 Updated nuclear data – ENDF/B-VIII.0

New ENDF/B-VIII.0 nuclear data libraries are available in COG 11.3 for continuous energy cross-sections (ENDFB8R0 and ENDFB8R0.ACE), probability tables for the unresolved resonance region (PT.ENDFB8R0.ACE), and thermal scattering laws (T.ENDFB8R0 and T.ENDFB8R0.ACE). Note that the ACE libraries were originally processed by Los Alamos National Laboratory using NJOY; whereas the library ENDFB8R0 was processed by the International Atomic

Energy Agency using PREPRO. The LLNL utility codes ACE2COG, ENDF2COG, and SAB2COG were then used to create the library files named above for direct use in COG.

### 2.2 Updated activation data – EAF-2010

The activation capabilities have been upgraded using EAF-2010 (the European Activation File 2010) and the ENDF-B-VIII.0\_decay (the ENDF/B-VIII.0 radioactive decay file) to generate a new COG 11.3 activation library, EAF-2010.

### 2.3 Advanced fission models – FREYA

Whereas ENDF/B-VII.1 had one average prompt neutron fission spectrum independent of incident neutron energy, ENDF/B-VIII.0 includes prompt neutron spectra and multiplicity dependent on the energy of the incident neutron causing fission. COG 11.3 also implements the latest version (2.0.4) of LLNL's advanced Fission Reaction Event Yield Algorithm (FREYA) [4]. FREYA provides additional fission physics including incident neutron-dependent and multiplicity-dependent spectra with angular correlations based on detailed sampling of the light and heavy fission fragments with pre-equilibrium

\* e-mail: [heinrichs1@llnl.gov](mailto:heinrichs1@llnl.gov)

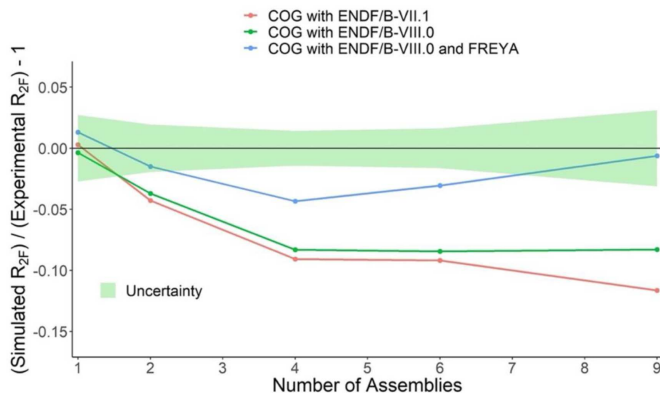


Fig. 1. ISSA R2F benchmark results.

neutron emission. In COG 11.3, FREYA is available for both CRITICALITY and SOURCE calculations in serial and parallel processing mode simply by adding the keyword *freya* to the BASIC block.

Nelson recently contributed a subcritical neutron multiplicity benchmark of LLNL's Inherently Safe Subcritical Assembly (ISSA) [5] to the International Criticality Safety Benchmark Evaluation Project (ICSBEP) [6]. R2F, the second moment of the count rate distribution normalized to the average count rate for infinite time gate size, is shown in Figure 1 to be quite sensitive to the degree of fission physics included in the simulation with ENDF/B-VIII.0 providing some improvement at the highest multiplication ( $M \approx 10$ ) corresponding to 9 assemblies and FREYA providing significant improvement overall. A summary paper [7] of this benchmark is available in the ICNC 2019 proceedings and additional benchmarks of this type are in preparation.

## 2.4 Time-tagged list-mode detector feature

A new OUTFILE option is available in COG 11.3, which creates a secondary output file listing the time, energy, and score of individual detector events. The default unit for time is seconds and for energy is MeV, but the outfile units can be changed in the BASIC block. This option is invoked by including in the DETECTOR description the line *outfile*. For example:

```
DETECTOR
number 1
reaction 2 1
mask-rea 1 40 $ scores only (n,pg) reactions
outfile
```

## 2.5 Spontaneous fission source features

In addition to the existing random emission time source option available in previous versions, COG 11.3 has a new feature for a spontaneous source for  $^{238}\text{U}$ ,  $^{238}\text{Pu}$ ,  $^{240}\text{Pu}$ ,  $^{242}\text{Pu}$ ,  $^{244}\text{Cm}$ , and  $^{252}\text{Cf}$  utilizing the full physics of FREYA. To define a spontaneous fission source simply include *particle-type sfs isotope* in the SOURCE block

under DEFINE ENERGY #, as shown in the example below.

```
SOURCE
npart 10000
define p 1
point 0. 0. 0.
define e 1
neutron sfs 98252
inc 1 p 1 e 1
```

This example yields an energy source of neutrons from spontaneous fission of  $^{252}\text{Cf}$  with multiplicity, energy, and direction as determined by FREYA. In the SFS mode, the first call for a source particle triggers a call to the FREYA event routine which returns the number and energies and directions of the neutrons generated by the spontaneous fission event. This data is stored in arrays. The first entry in these arrays is the energy and direction of the first particle, the second entry gives the energy and direction of the second source particle, and so on. COG transports these particles one by one until the array is empty, at which time the FREYA event routine is called again to fill the arrays and the process is repeated.

A second more complete spontaneous fission source is also available. To define this complete spontaneous fission source simply include *particle-type fsssrc isotope* in the SOURCE block under DEFINE ENERGY #, as shown in the example below.

```
SOURCE
npart 10000
define p 1
point 0. 0. 0.
define e 1
neutron fsssrc 98252
Inc 1 p 1 e 1
```

In the FissSrc mode, a call for a source particle again triggers the FREYA event routine which returns the number and energies and directions of the particles (neutrons in the above example) generated by the spontaneous fission event. Rather than releasing these particles one at a time as in the SFS mode, they are released as a packet with the same generation time and with correlated energies and directions. In the example above, the *particle type* is neutron which yields a neutron-only source. A *particle-type* of a photon (or gamma) would yield a photon-only source, and a *particle-type* of neut-pho would yield a neutron-photon source.

## 2.6 Effective delayed neutron fraction calculation

To assist users in critical assembly design and reactor physics, COG 11.3 has three estimators for the effective delayed neutron fraction, beta-eff, or  $\beta_{\text{eff}}$ . The first is simply the ratio of the number of fissions produced by delayed neutrons divided by the total number of fissions produced by all neutrons [8]. The second is simply the ratio of the number of fission neutrons produced by delayed neutrons divided by the total number of fission neutrons produced by all neutrons [9]. The third estimator is the prompt method [10] estimated as  $1 - (k_p/k_{\text{eff}})$  where  $k_{\text{eff}}$  is the

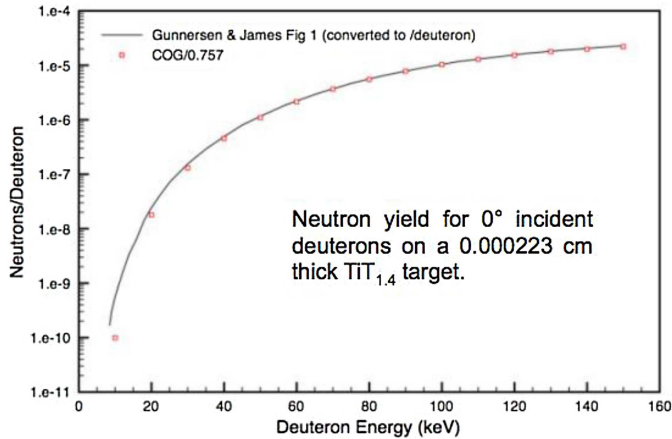


**Fig. 2.** Calculated neutron yield from deuterons on a titanium-tritium target.

effective neutron multiplication factor and  $k_p$  is the effective prompt neutron multiplication factor. Sample results for these estimators are given in Table 1, which are in agreement with experimental errors. These and additional results are published [10]. Note that where no uncertainty is provided in Table 1, this uncertainty is insignificant, i.e., less than 0.5 pcm.

### 2.7 Alpha particle transport

Alpha particle transport is available in COG 11.3. The results of COG calculations with comparison to experimental thick target yields, and comparison to the AlfaMC code results, are published [11].

### 2.8 Deuteron particle transport

Deuteron particle transport is also available in COG 11.3. The results of COG calculations on neutron yield and spectra are in good agreement with published results [12,13] as shown in Figures 2–3.

### 2.9 General lattice features

A new pre-processor has been added to COG to read and process a string of data between the braces {} within a UNIT definition to generate and automatically run a new input file with the suffix .cnvrt.

#### 2.9.1 Rectangular lattice

If the first symbol in the {} is “x” then the data represents a rectangular lattice which is a UNIT containing a general three-dimensional lattice constructed of multiple USE UNIT statements centered between X, Y, and Z planes defined in the string in a specified arrangement.

In the example given below, sixteen planes are created and numbered at equal spacing from 1501 PLANE X -6.00075 to 1516 PLANE +6.00075, and similarly from

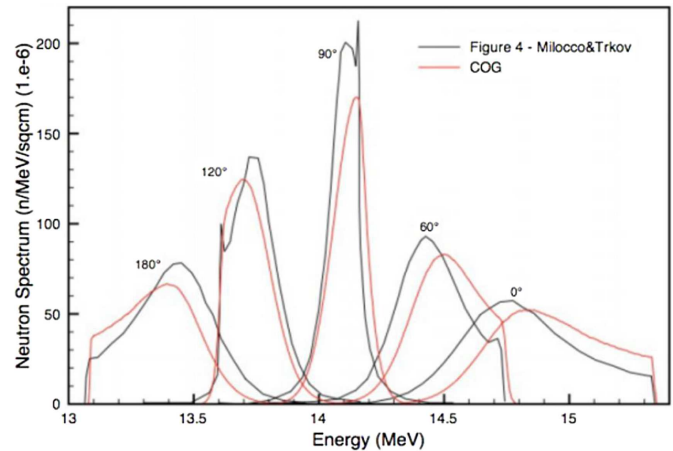


**Fig. 3.** Calculated neutron spectra from deuterons on a titanium-tritium target.

1601 PLANE Y -6.00075 to 1616 PLANE +6.00075. Two planes are specified from 1701 PLANE Z -70. to 1702 PLANE +70. Within the  $15 \times 15 \times 1$  spaces defined within  $16 \times 16 \times 2$  planes, a series of USE UNIT statements are generated per the patten below in which each unit 1 or 2 is centered between the planes.

```

DEFINE UNIT 3 $ 15 x 15 x 1 array of fuel assemblies
{ x 1501 16 [-6.00075 6.00075]
  y 1601 16 [-6.00075 6.00075]
  z 1701 -70. 70.
  fill
  1 1 1 1 1 1 1 1 1 1 1 1 1 1 1
  1 1 1 1 1 1 1 1 1 1 1 1 1 1 1
  1 1 2 1 1 2 1 1 1 2 1 1 2 1 1
  1 1 1 1 1 1 1 2 1 1 1 1 1 1 1
  1 1 1 1 2 1 1 1 1 1 2 1 1 1 1
  1 1 2 1 1 2 1 1 1 2 1 1 2 1 1
  1 1 1 1 1 1 1 1 1 1 1 1 1 1 1
  1 1 1 2 1 1 1 2 1 1 1 2 1 1 1
  1 1 1 1 1 1 1 1 1 1 1 1 1 1 1
  1 1 2 1 1 1 1 1 1 1 1 1 2 1 1
  1 1 1 2 1 1 1 1 1 1 1 2 1 1 1
  1 1 1 1 1 1 1 2 1 1 1 1 1 1 1
  1 1 2 1 1 2 1 1 1 2 1 1 2 1 1
  1 1 1 1 1 1 1 1 1 1 1 1 1 1 1
  1 1 1 1 1 1 1 1 1 1 1 1 1 1 1 }
    
```

#### 2.9.2 X-oriented triangular lattice

If the first symbol in the {} is “tri-x” then the data represents an x-oriented triangular lattice. The following is a graphical representation of a  $3 \times 5 \times 1$  x-triangular lattice.

```

1st point> 1 1 1
           1 2 1
           2 2 2
           1 2 1
-----x  1 1 1
2nd point ^ ^3rd point
    
```

Four sets of planes are generated: equally spaced x-planes, equally spaced positive-slope planes, equally

**Table 1.** Sample COG 11.3 calculated beta-eff results with ENDF/B-VIII.0 (in pcm).

Sample	Experiment	First estimator	Second estimator	Third estimator
NASA ZPR-1 H/X=565	$820 \pm 40$	794	794	$794 \pm 1$
TCA 2.48U $16 \times 16$	$765 \pm 18$	764	759	$757 \pm 5$
Godiva	$659 \pm 28$	679	647	$642 \pm 4$
FCA XIX-2	$364 \pm 9$	372	366	$364 \pm 8$
FCA XIX-3	$251 \pm 4$	258	254	$253 \pm 7$
Jezebel	$195 \pm 10$	197	184	$183 \pm 5$

spaced negative-sloped planes, and two  $z$ -planes. These planes define nested cells of hexagonal prisms. In the example below,  $-3. 3.$  are the  $x$ - $y$  coordinates of the center of the upper left cell,  $-5. -3.$  are the coordinates of the center of the lower left cell,  $0. -3.$  are the  $x$ - $y$  coordinates of the center of the lower right cell,  $3 5 1$  are the number of cells per row, the number of cells per column, and the number of cells stacked axially,  $-70. 70.$  are the bounding  $z$ -planes,  $101 201 301 401$  are the initial numbers for the four sets of planes, and `fill` is a keyword indicating that the next entries are the unit numbers filling the array left-to-right, top-to-bottom.

```

DEFINE UNIT 5 $ 3 x 5 array
{ tri-x
-3. 3.
-5. -3.
0. -3.
3 5 1
-70. 70.
101 201 301 401
Fill
1 1 1
1 2 1
2 2 2
1 2 1
1 1 1 }

```

### 2.9.3 Y-oriented triangular lattice

If the first symbol in the `{}` is “`tri-y`” then the data represents a  $y$ -oriented triangular lattice. The following is a graphical representation of a  $5 \times 3 \times 1$   $y$ -triangular lattice.

```

1st point> 1 1 1
y          1 2 1
|           2 2 2
|           1 2 1
---x      1 1 1
2nd point ^ 3rd point

```

Four sets of planes are generated: equally spaced  $y$ -planes, equally spaced positive-slope planes, equally spaced negative-slope planes, and two  $z$ -planes. These planes define nested cells of hexagonal prisms. In the example below,  $-3. 5.$  are the  $x$ - $y$  coordinates of the center of the upper left cell,  $-3. 0.$  are the coordinates of the center of the lower left cell,  $3. -5.$  are the  $x$ - $y$  coordinates of the center of the lower right cell,  $5 3 1$  are the number

of cells per row, number of cells per column, and number of cells stacked axially,  $-70. 70.$  are the 2 bounding  $z$ -planes,  $101 201 301 401$  are the initial numbers for the four sets of planes, and `fill` is a keyword indicating that the next entries are the unit numbers filling the array top-to-bottom, left-to-right.

```

DEFINE UNIT 6 $ 5 x 3 array
{ tri-y
-3. 5.
-3. 0.
3. -5.
5 3 1
-70. 70.
101 201 301 401
Fill
1 1 2 1 1
1 2 2 2 1
1 1 2 1 1 }

```

These features have proven very useful and have been extensively utilized in modeling ICSBEP criticality benchmarks and in criticality safety evaluations of large interacting arrays.

## 2.10 New parallel processing capabilities

The existing ALPHA (i.e., the inverse reactor period) and CritDetVR features, only available in serial processing mode in previous versions, are now available for parallel processing using MPI in COG 11.3.

## 2.11 Updated electron transport capabilities

Electron transport in COG 11.3 has been upgraded from EGS4 to EGS5 [14] together with the capability to now call PEGS5 directly from within COG to generate the required EGS5 data library.

## 2.12 New imaging detector

A new imaging detector feature has been added as a standard feature in COG 11.3 based on an external USERDET feature originally developed by Dr. James Hall. A User Guide [15] describing this feature is published as is a detailed comparison of COG 11.3 to MCNP6.2 sample calculations [16].

### 2.13 Modernized COG website

The COG website, <https://cog.llnl.gov>, has been updated and modernized. The top-level page provides a brief description of the code and identifies the twelve particles currently supported as well as information on how to obtain the code and contact the developers using the email address [cog@llnl.gov](mailto:cog@llnl.gov). The Publications subpage includes a new search filter based on a keyword or string of keywords. The Registration page has been simplified and all users are encouraged to register. The training webpage contains tutorial documentation as well as information on how to request a training session or course. Lastly, a new subpage devoted to software quality assurance (SQA) is intended to expedite internal and regulatory reviews of compliance with 10 CFR 830, DOE O 414.1D, and NQA-1; and provides users with a comprehensive repository of verification and validation (V&V) test results.

## 3 Conclusion

COG 11.3 is the culmination of 10 years of development since the previous public release and represents the authors' commitment to providing users access to the latest nuclear data libraries, advanced physics models, and implementation of new particles, geometry, source, and detector features per user requests.

### Acknowledgments

This paper is dedicated to Dr. Richard M. Buck, who retired from the COG code development team in September 2017.

### Funding

This work was performed under the auspices of the U. S. Department of Energy by Lawrence Livermore National Laboratory under contract DE-AC52-07NA27344 with sponsorship of the U. S. Department of Energy Nuclear Criticality Safety Program.

### Conflicts of interest

The authors declare that they have no competing interests to report.

### Data availability statement

Data associated with this article are available from <https://cog.llnl.gov>

### Author contribution statement

David Heinrichs is the Nuclear Criticality Safety Division Leader at LLNL and responsible manager for COG software. Edward Lent is the Principal Computational Physicist for COG software. Chuck Lee is the Principal Computer Scientist for COG software.

## References

1. D. Heinrichs, S. Kim, D. Biswas, et al., COG 11.1 Code Features for Shielding and Criticality Safety Analysis, LLNL-PROC-642136, Lawrence Livermore National Laboratory, August 15, 2013
2. R. Buck, D. Cullen, D. Heinrichs, et al., COG – Publicly Available Now to Criticality Safety Practitioners, in *Proceedings of the 8th International Conference on Nuclear Criticality Safety, St. Petersburg, Russia, 2007* (2007)
3. R. Buck, D. Heinrichs, A. Krass, et al., COG – Special Features of Interest to Criticality Safety Practitioners, *Trans. Am. Nucl. Soc.* **102**, 305 (2010)
4. J. Verbeke, J. Randrup, R. Vogt, FREYA 2.0: New Developments in Fission Chain Modeling, in *Proceedings of the Institute for Nuclear Materials Management Annual Meeting, Palm Desert, CA, USA, July 2017* (2017)
5. D. Heinrichs, J. Burch, B. Hudson, et al., Design, Development and Utilization of the New LLNL Inherently Safe Subcritical Assembly (ISSA), LLNL-CONF-670257, Lawrence Livermore National Laboratory, May 4, 2015
6. A. Nelson, S. Kim, J. Verbeke, et al., Subcritical Measurements of Water-Moderated Highly Enriched Uranium Oxide MTR Type Fuel, NEA/NSC/DOC/(95)03IX, FUND-LLNL-ALPHAN-HE3-MULT001, Rev. 0, Nuclear Energy Agency, OECD, May 31, 2019
7. A. Nelson, W. Monange, S. Kim, et al., Fundamental Physics Subcritical Neutron Multiplicity Benchmark Experiments Using Water Moderated Highly Enriched Uranium Fuel, LLNL-CONF-778008, Lawrence Livermore National Laboratory, June 14, 2019
8. R. Meulekamp, S. van der Marck, Calculating the Effective Delayed Neutron Fraction with Monte Carlo, *Nucl. Sci. Eng.* **152**, 142 (2006)
9. S. Pearlstein, The Effective Delayed Neutron Fraction for Bare-Metal Criticals, *Nucl. Tech.* **128**, 482 (1999)
10. D. Heinrichs, E. Lent, W. Zywiec, COG Beta-Effective Benchmarks, LLNL-TR-843852, Lawrence Livermore National Laboratory, December 20, 2022
11. E. Lent, Alpha Transport in COG, LLNL-TR-655365, Lawrence Livermore National Laboratory, June 4, 2014
12. E. Gunnerson, G. James, On the Efficiency of the Reaction  $H^3(d,n)He^4$  in Titanium Tritide Bombarded with Deuterons, *Nucl. Instr. Meth.* **8**, 173 (1960)
13. A. Milocco, A. Trkov, Modelling of the Production of Source Neutrons from Low-Voltage Accelerated Deuterons on Titanium-Tritium Targets, *Sci. Technol. Nucl. Install.* **2008**, 340282 (2008)
14. H. Hirayama et al., The EGS5 Code System, SLAC-R-730, KEK-2005-8, January 13, 2016
15. M.-A. Descalle, COG Imaging Detector User Guide by Jim Hall and Ed Lent, LLNL-PRES-843321, Lawrence Livermore National Laboratory, May 14, 2020
16. J. Hall, Neutron Image Simulations – MCNP6 vs. COG11, LLNL-PRES-831931, Lawrence Livermore National Laboratory, February 2022